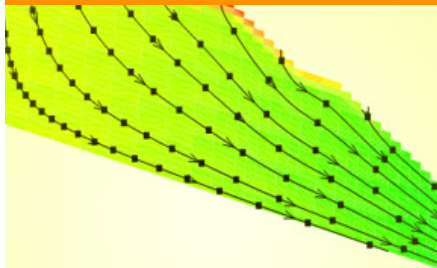


## Original Research



A fatal accident at a mine waste rock dump was thought to be due to the downward flow of  $O_2$ -deficient air originating from the dump. A numerical model tested the plausibility of various physical mechanisms hypothesized to control gas flow in the dump. The main initial hypotheses were that gas flow leading to the incident was due to the sole or combined effect of changes in barometric pressure, temperature, or till cover water saturation.

B. Lahmira and R. Lefebvre, Institut National de la Recherche Scientifique (INRS), Centre-Eau Terre Environnement, Québec, QC, G1K 9A9, Canada; D. Hockley, SRK Consulting (Canada) Inc., Vancouver, BC, V6E 3X2, Canada; and M. Phillip, O'Kane Consultants USA Inc., Anaconda, MT 59711. \*Corresponding author (belkacem.lahmira@gmail.com).

Vadose Zone J.  
doi:10.2136/vzj2014.03.0032  
Received 31 Mar. 2014.

© Soil Science Society of America  
5585 Guilford Rd., Madison, WI 53711 USA.

All rights reserved. No part of this periodical may be reproduced or transmitted in any form or by any means, electronic or mechanical, including photocopying, recording, or any information storage and retrieval system, without permission in writing from the publisher.

# Atmospheric Controls on Gas Flow Directions in a Waste Rock Dump

Belkacem Lahmira,\* René Lefebvre, Daryl Hockley, and Mark Phillip

The Sullivan Mine No. 1 Shaft waste rock dump was built on a natural slope and covered by till. The outflow of  $O_2$ -deficient gas through a leachate drainage pipe in an enclosure at the base of the dump resulted in four fatalities. A numerical model was developed to understand the mechanism controlling gas flow, which was found to be the relative buoyancy of the gas phase within the dump compared with atmospheric air. Changes in atmospheric air density are caused by atmospheric temperature variations, whereas dump gas-phase density is relatively constant due to a steady internal dump temperature. When the air temperature is lower than the internal dump temperature, atmospheric air density is higher than the dump gas density, inducing upward dump gas flow and air entry into the drainage pipe. Downward dump gas flow occurs and exits the drainage pipe when high atmospheric temperature leads to an air density lower than the dump gas density. A gas flow behavior similar to what was observed at the No. 1 Shaft dump could occur in other covered dumps.

Abbreviations: AMD, acid mine drainage.

**A fatal accident** occurred in May 2006 at the No. 1 Shaft waste rock dump of the Sullivan Mine, BC, Canada. This accident was thought to be related to the downward flow of  $O_2$ -deficient air originating from the waste dump. That air was presumed to have entered a water sampling enclosure located at the base of the waste dump through the water sampling pipe. We developed a numerical model whose objective was to test the plausibility of various physical mechanisms that were hypothesized to be controlling gas flow in the Sullivan Mine No. 1 Shaft waste dump. The main initial hypotheses were that gas flow leading to the fatalities incident could have been related to the sole or combined effect of changes in barometric pressure, temperature, or till cover water saturation. Dawson et al. (2009) and Phillip et al. (2009) provided a full description of the site, the characterization program performed to determine material properties and conditions prevailing in the dump, and the monitoring program that followed gas flow through the water sampling pipe as well as conditions in the dump related to variations in atmospheric temperature and pressure.

The Sullivan Mine, now closed and reclaimed, is located adjacent to Kimberley, BC, Canada. Figure 1 shows the No. 1 Shaft waste rock dump, which was built from 1950 to 2001, principally by the deposition of waste rock from the No. 1 Shaft. A very low permeability bedrock, compared with the waste rock, makes up the base and slope. Waste rock was deposited along the natural slope on bedrock to attain a total height of approximately 55 m. The dump was resloped and covered with a 1-m till layer. The fatalities occurred in the monitoring station located at the southeast corner of the dump toe, where a 40.6 cm (16 inch) diameter pipe conveys acid mine drainage (AMD) leachate toward the site water treatment system. Figure 1 also shows the location of the main instrumentation used to characterize and monitor the waste rock dump: (i) inward and outward gas velocity, composition ( $O_2$  and  $CO_2$ ), and temperature are measured

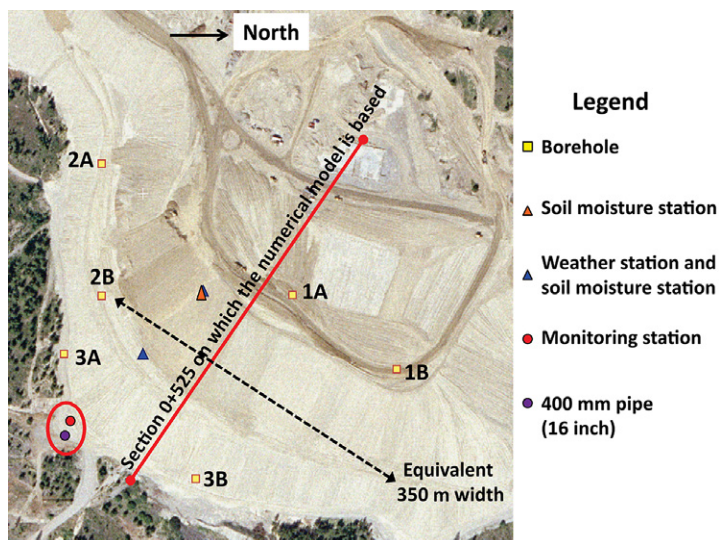


Fig. 1. Site map of the waste rock pile based on an aerial photograph. The site instrumentation is shown, including the instrument shed with data recording equipment (red circle) for the monitoring station containing the drainage pipe (purple circle). Location of Section 0+525 used to develop the numerical grid is also shown. (Figure modified from Dawson et al., 2009).

in the pipe; (ii) boreholes are instrumented with thermistors and gas tubes, allowing the monitoring of temperature and gas pressure and the regular sampling of dump gas; (iii) a weather station measures air temperature and relative humidity, wind speed and direction, precipitation, and net radiation; and (iv) soil temperature and volumetric water content are measured at different depths in the till cover. The characterization and monitoring program performed at the No. 1 Shaft waste rock dump were fully described by Phillip et al. (2009). Figure 1 also shows the location of Section 0+525 used as a basis for the development of the two-dimensional vertical cross-section numerical model described below (Fig. 2).

## Gas Flow in Waste Rock Dumps

### Gas Buoyancy and Pneumatic Potential Controlling Gas Flow

Kuang et al. (2013) recently reviewed air flow in the unsaturated zone. In this review, they presented the state of knowledge on subsurface airflow induced by natural forcings and discussed the process of induced airflow. Governing equations and numerical models as well as field and laboratory experimental results were also presented. Gas flow can be generated by gradients in gas pressure, temperature, or composition (Lefebvre et al., 2001a; Lefebvre, 2010, Chapter 4). All these mechanisms can potentially contribute to gas flow in a waste rock dump. In these systems, density-driven air convection and thermal conduction are the most significant transport mechanisms (Lu and Zhang, 1997; Lefebvre et al., 2001a). The rate of gas flow within the piles directly affects the

O<sub>2</sub> supply and the thermal state of the waste rock piles (Chi et al., 2013; Pham et al., 2013).

Convective gas flow within permeable and unsaturated materials is known to occur whenever there is a sufficient temperature contrast between the deeper soil and the atmosphere, which creates an air density gradient (Guo, 1993; Lefebvre et al., 2001b, 2011; Lahmira et al., 2009; Lahmira, 2010; Kamai et al., 2009; Nachshon et al., 2008; Weisbrod et al., 2009; Weisbrod and Dragila, 2006). Heat production related to highly exothermic sulfide oxidation increases the temperature and thus leads to thermal gas convection and subsequent changes in O<sub>2</sub> fluxes within the waste rock (Lahmira et al., 2007; Lahmira, 2010; Lahmira and Lefebvre, 2014). Ganot et al. (2012), in a different context, showed a similar impact of thermal convection on air circulation and O<sub>2</sub> supply in a mammalian burrow under arid conditions. Similarly, Lahmira et al. (2014) showed that the convective air flow through a reclamation cover over an unsaturated coke dump at an oil sands mine can have an impact on the water distribution within the cover, resulting in additional moisture losses beyond those expected by evapotranspiration, thus causing accelerated drying of the cover. An analogous process occurs in regions of fractured soil surfaces, where water vapor escaping through fractures affects soil respiration by changing the soil moisture conditions (Weisbrod et al., 2009; Kamai et al., 2009).

Barometric pressure changes can also generate pressure gradients between the gas present in a waste rock dump and the atmosphere, which causes gas exchanges with the atmosphere by compression or expansion of the dump gas column (Wels et al., 2003; Smolensky et al., 1999). Furthermore, temporal fluctuations in barometric pressure can trigger the mechanism of convection and significantly enhance gas migration (Massmann and Farrier, 1992; Massman and Frank, 2006). Such gas pressure fluctuations within the unsaturated zone due to barometric pressure changes have been used in some studies to determine air permeability in the unsaturated zone (Weeks, 1979; Smolensky et al., 1999; Neeper, 2002; Wu et al., 2006). Barometric flow in boreholes themselves was the subject of studies for the purpose of extracting contaminant vapor (Neeper, 2003; Neeper and Stauffer, 2005). Finally, pressure gradients can be induced by wind flow over a rock pile, thus causing more air flow into the pile (Anne and Pantelis, 1997; Ritchie and Miskelly, 2000; Amos et al., 2009; Nachshon et al., 2012), which can result in higher maximum temperature in materials containing reactive sulfides (Moghtaderi et al., 2000). A similar process was studied by Nachshon et al. (2008, 2012), who quantified the effect of ground-surface wind and a thermal gradient on convective ventilation of fractures and its subsequent impact on earth-atmosphere air circulation.

Gas exchanges between the atmosphere and an unsaturated waste rock pile in a permafrost environment are controlled by similar processes but involve distinct behaviors. The physical and geochemical processes controlling AMD generation in waste rock piles were

studied in a complete and multidisciplinary project conducted at the Diavik mine (Northwest Territories, Canada) (Chi et al., 2013; Smith et al., 2013a, 2013b, 2013c; Neuner et al., 2013; Bailey et al., 2013; Pham et al., 2013). Chi et al. (2013) showed that advection driven by the wind-induced pressure on the surface was the dominant gas transport process within the Diavik test pile. Pham et al. (2013) showed that the wind-driven gas transport is significantly enhancing thermal transport rates and produces rapid responses (compared to conduction) to changes in ambient temperatures due to wind and natural air convection.

Chemical reactions in dumps can consume  $O_2$  related to sulfide oxidation and release  $CO_2$  by carbonate dissolution, which can alter the molar mass and density of the dump gas phase, leading to gas flow related to positive or negative dump gas buoyancy relative to the atmospheric air. The presence of water vapor in the gas phase also has an effect on its density. In this study, we considered that all gas phases were saturated in water vapor and assessed their density accordingly. Furthermore, these three gas flow mediators (gas pressure, temperature, and composition) are not independent because, for example, gas temperature or composition changes can alter the gas pressure.

In the present study, monitoring data and results from the numerical modeling of the No. 1 Shaft waste rock dump discussed below show the key role of atmospheric temperature on dump gas flow. We thus explain first the physical process dependent on temperature that can be at the origin of gas flow. The principles of thermal convection due to dump gas buoyancy discussed here will facilitate the explanation of the numerical modeling results presented below.

Dump gas buoyancy depends on its density relative to atmospheric air. Gas (or air) density  $\rho_a$  ( $kg\ m^{-3}$ ) is obtained from the following relations derived from the gas law (Lefebvre, 2010, Eq. [3.7], p. 95):

$$\rho_a = \frac{M}{V} = \frac{nm}{V} = \frac{pm}{RT'} = \frac{p \sum (x_i m_i)}{RT'} \quad [1]$$

where  $M$  (kg) and  $V$  ( $m^3$ ) are the mass and volume of gas, respectively. The mass of gas depends on its number of moles  $n$  (mol) and its molar mass  $m$  ( $kg\ mol^{-1}$ ). The molar mass of a gas such as atmospheric air, which is a mixture of  $i$  components, is the sum of the products of molar fractions  $x_i$  and the molar masses  $m_i$  of these components. The volume of gas is obtained from its pressure  $p$  (Pa), absolute temperature  $T'$  (K), and the gas constant  $R$  ( $8.31\ Pa\ m^3\ mol^{-1}\ K^{-1}$ ).

In the case of the No. 1 Shaft dump, the presence of  $CO_2$  in the dump gas compensates for the loss of  $O_2$  so that the molar mass of dump gas is globally very similar to that of atmospheric air (Lahmira and Lefebvre, 2008). Also, under steady-state equilibrium, the mean gas pressure is fixed at a similar value by the

prevalent barometric pressure both in the atmosphere and within the dump. The difference between dump gas and atmospheric air densities thus depends only on their respective temperatures, gas density being inversely proportional to temperature.

At depths between 5 and 30 m, the dump maintains a relatively steady mean internal temperature of about 10 to 12°C that it imparts to the gas phase present within the dump (temperature profiles can be found in Lahmira and Lefebvre, 2008). However, the atmospheric temperature is quite variable, so that the density of the atmospheric air in contact with the dump will vary. Based on these principles and as shown below by the simulation results, in the case where the atmospheric temperature is similar to the mean dump temperature, the density of the atmospheric air will be the same as that of the dump gas and there will be no tendency for dump gas to flow. This is referred to here as the *equilibrium temperature*. However, when the atmospheric temperature is lower than the dump temperature, its density is higher than that of the dump gas, which will tend to rise up through the dump (positive buoyancy). On the contrary, when the atmospheric temperature is higher than the dump temperature, its density is lower than that of the dump gas, which will tend to sink down through the dump (negative buoyancy).

This process of buoyancy-driven gas flow controlled by atmospheric temperature differences from the dump equilibrium temperature is in agreement with the measured directions and magnitudes of pipe gas velocity vs. atmospheric temperature (Fig. 3), as discussed below. For this gas circulation process to occur, there has to be flow through the till cover and waste rock in the dump to maintain continuous flow. The pipe directly connects the dump to the atmosphere at its lower end, but flow also has to go through the dump top surface or through defects in the till cover to maintain flow in the upper end. Dawson et al. (2009) provided pictures and a section showing the 400-mm drainage pipe connecting a former drainage ditch, now filled with coarse drain rock, to the base of a monitoring station. The drainage ditch was filled to provide more space to reslope the pile and lay a till cover on its surface. Waste rock and the till cover were thus extended over the former drainage ditch. The till cover restricts gas flow, but the pipe provides direct access between the waste rock and the atmosphere at the base of the dump. If the till cover were perfectly impermeable, gas flow would not be sustainable. The dump would then behave like a sealed container connected to the atmosphere only through the pipe. Pressure equilibration between dump gas and the atmosphere would then occur only by gas circulation through the pipe, and there would be zero gas flow through the pipe or dump at steady state after pressure equilibration. Furthermore, flow through the pipe would then be linked to barometric pressure changes, rather than atmospheric temperature variations. Thus, the strong relation of pipe gas velocity with atmospheric temperature and the insignificant effect of barometric pressure (Phillip et al., 2009) provide strong indirect evidence that significant gas flow can occur through the dump surface.



The magnitude of dump gas flow through the dump is driven by the difference in the pneumatic potential between the top and base of the dump, which is caused by the buoyancy of dump gas relative to atmospheric air. The numerical simulator rigorously takes into account all processes contributing to gas flow as well as the compressibility of the gas phase. However, the simulator does not provide as an output the values of the pneumatic potential. These potentials are much better for showing the processes controlling dump gas flow and gas exchanges between the dump and atmosphere than gas pressure. Thus, for the purpose of generating meaningful graphs, the following simplified form of the pneumatic potential  $\Psi$  (Pa) was calculated using the numerical modeling results (Lefebvre, 2010, Eq. [2.4], p. 42):

$$\Psi = \rho g(z - z_0) + p \quad [2]$$

Equation [2] is analogous to the definition of hydraulic head, with a component of gas pressure  $p$  (Pa) and a component of elevation, which is the product of gas density  $\rho$  ( $\text{kg m}^{-3}$ ), gravitational acceleration  $g$  ( $9.81 \text{ m s}^{-2}$ ), and the elevation difference between the pressure measurement point  $z$  (m) and an arbitrary reference elevation  $z_0$  (m) (elevation is positive upward). This relationship neglects gas compressibility, i.e., the fact that density varies with pressure, as shown by Eq. [1]. However, within the short vertical interval of the No. 1 Shaft dump, there is only a very small change in density related to elevation and pressure. Pneumatic potentials were thus calculated inside the dump using the mean dump gas density corresponding to the mean internal dump temperature and pressure. The same relationship was also used for the surface boundary elements corresponding to atmospheric conditions. Pneumatic potentials for boundary atmospheric conditions indicate if atmospheric pneumatic potentials are in equilibrium with the dump gas or would instead induce upward or downward dump gas flow.

## General Waste Rock Dump Numerical Modeling Approach

The numerical simulator TOUGH AMD was used to develop a model representing the No. 1 Shaft waste rock dump. TOUGH AMD represents multiphase transfer processes and reactions within acid-generating rock piles containing pyrite (Lefebvre, 1994; Lefebvre et al., 2001a, 2001b). It is based on the general multiphase, nonisothermal, and multicomponent simulator TOUGH2 (Pruess, 1991; Pruess et al., 2012). The numerical simulator TOUGH AMD considers an energy component (heat) and three mass components: water and air subdivided into two components ( $\text{O}_2$  and other air gases). Pyrite oxidation has first-order kinetics relative to  $\text{O}_2$ . A reaction core model represents the pyrite oxidation kinetics in mine rock and the  $\text{O}_2$  loss and heat production resulting from the oxidation as a function of temperature,  $\text{O}_2$  concentration, and pyrite mass fraction. TOUGH AMD has been used to simulate physical processes related to AMD-producing waste rock piles at other sites (Wels et al., 2003; Sracek et al., 2004; Lefebvre, 1995; Lefebvre and G  linas, 1995; Lefebvre et al., 1998,

2001b, 2001c, 2002; Smolensky et al., 1999; Lahmira and Lefebvre, 2008, 2014; Lahmira et al., 2009, 2014; Lahmira, 2010).

The number of unknowns needed to specify the state of a numerical system depends on the number of phases and components considered (Pruess et al., 2012). Waste rock dumps in which AMD is occurring are partially water-saturated porous media within which  $\text{O}_2$  consumption occurs due to sulfide oxidation (mostly pyrite), which leads to heat production (Lefebvre et al., 2001a). Numerical simulation of AMD in waste rock dumps thus involves the simultaneous estimation of four unknowns to determine the state of the system (gas pressure, water saturation, mass fraction of  $\text{O}_2$ , and temperature). The simulator also has to calculate the equation of state defining the equilibrium concentrations of the components (water, air, and  $\text{O}_2$ ) in the two fluid phases (gas and liquid) as a function of temperature. This numerical problem is thus demanding, so that detailed numerical grids would require a long computation time to solve for the transient evolution of the system. For the numerical simulation of AMD production in waste rock, it is thus normally preferred to use relatively coarse grid elements, while capturing the most important features of the dump geometry and material distribution (Lefebvre et al., 2001b).

For the simulations in this study, the direct numerical solver of TOUGH2 was used. Although not as efficient as indirect solvers, the direct solver is extremely robust and can handle very coarse grids and drastic changes in properties between adjacent elements. TOUGH2 capabilities have been used to tackle a wide range of demanding numerical problems, including free convection due to variable fluid densities related to large salt concentrations or the injection of  $\text{CO}_2$  (Pruess, 1991; Pruess et al., 2012; Finsterle and Sonnenthal, 2012; <http://esd.lbl.gov/research/projects/tough/>).

## Simplifying Assumptions for the No. 1 Shaft Dump Modeling

Key processes assumed to exert the most important controls on gas flow were to be the focus of initial numerical simulations, using simplified conditions. It was planned to later develop a model with more complex conditions to consider expected departures from the simplified model relative to the observed conditions. Compared with the general case of AMD in waste rock, the conditions prevailing in the No. 1 Shaft dump at the Sullivan Mine allow the modeled system to be simplified as follows:

- Thermal conditions: Isothermal (fixed temperature) conditions could be used but with different temperatures assigned to the dump and atmosphere, without considering heat transfer, thus avoiding the need to solve for temperature.
- Gas composition: Fixed gas composition, equivalent to atmospheric air, was assigned to gas phases in the dump and atmosphere, thus avoiding the need to solve for gas composition.
- Water flow: Fixed water saturations, at different values for the waste rock and till cover, were imposed as residual water. This implies that no liquid water flow is represented, thus avoiding

the solution of highly nonlinear liquid flow under unsaturated conditions.

Isothermal conditions could be used because it was shown that the average temperature in the No. 1 Shaft dump is relatively uniform and remains relatively constant throughout the year below a depth of about 5 to 7 m, compared with the total thickness of waste rock on the order of 20 m. Lahmira and Lefebvre (2008) provided graphs of the measured temperature profiles. The internal dump temperature is thus relatively independent of atmospheric conditions. Different simulations were thus performed with a fixed temperature assigned to the waste rock but at different values of atmospheric temperature in contact with the dump surface. However, because the simulator cannot represent temperatures  $<0^{\circ}\text{C}$ , involving water freezing, in the numerical simulations the mean dump temperature was shifted upward as well as the atmospheric temperatures representing the range of variations observed at the site.

A fixed gas composition can be imposed in the numerical model because the dump gas phase was shown to have a mean molar mass similar to that of the atmospheric air (Lahmira and Lefebvre 2008). Although the dump gas phase is deficient in  $\text{O}_2$ , which would lower the molar mass, it contains a proportion of  $\text{CO}_2$  that brings its molar mass close to that of atmospheric air. Atmospheric air contains 21% (v/v)  $\text{O}_2$  and 0.03% (v/v)  $\text{CO}_2$  and other atmospheric gases, with a mean relative humidity of 70% at the site, which leads to a humid gas molar mass of  $0.0288 \text{ kg mol}^{-1}$ . The dump gas phase contains atmospheric gases but is partially depleted in  $\text{O}_2$  (3–5% v/v), whereas it has a larger than atmospheric proportion of  $\text{CO}_2$  (4–5% v/v) and is fully saturated in water vapor at mean dump temperatures ranging from 10 to  $14^{\circ}\text{C}$ . The dump gas composition leads to a humid gas molar mass of  $0.0287 \text{ kg mol}^{-1}$ , which is almost identical to atmospheric air. Under such conditions, the dump gas-phase composition will not significantly influence its density relative to atmospheric air. Using the same equivalent composition for both gas phases should thus lead to representative gas flow. This simplifying assumption avoids the need to represent  $\text{O}_2$  consumption related to AMD production due to sulfide oxidation.

The dump is a partially water-saturated medium in which there is slow water infiltration, first through the till cover and then through the underlying waste rock. However, the presence of the low-permeability till cover spreads water flow relatively evenly throughout the year, even though it may vary seasonally, being expected to be higher during and following the spring snowmelt. Such conditions result in relatively stable water saturations whose influence on gas flow should remain quite constant throughout the year. Thus, including the solution of water flow in the system would not enhance the representation of gas flow. To impose water saturations representative of the system in the till cover and waste rock, while keeping water immobile, residual water

saturation values were increased in the numerical model above imposed water saturations for each material. Under these conditions, the permeabilities of the materials used as input in the numerical model correspond to effective air permeabilities controlling gas flow. Still, to take into account the effect of varying water saturation in the till cover, two simulation scenarios were used to represent “wet” and “dry” water saturation in the till cover and their corresponding effective permeabilities. Based on field monitoring data, water saturation in the till cover for those conditions were both quite high, being at 95 and 80%, respectively. Since results obtained for simulations with different saturations in the till were quite similar, only results for the case corresponding to the dry till cover are presented here.

TOUGH AMD actually has capabilities that would allow simulations without using these simplifications. However, simulation results obtained using the simplified conditions showed that the system behavior could be explained quite well without considering more complex processes.

## ◆ Numerical Model Development and Validation

### Numerical Modeling Program

For the numerical simulation of gas flow in the No. 1 Shaft waste rock dump, different emphasis was placed on the representation of the three potential gas flow processes. As explained above, gas flow related to gas composition changes was neglected a priori based on available data showing that the dump gas molar mass is equivalent to that of the atmospheric air. Special emphasis was placed on the representation of the effect of atmospheric temperature on dump gas flow because pipe gas velocity monitored at the site was observed to be strongly correlated to the atmospheric temperature. Figure 3 shows gas velocity monitoring data measured in the partially air-filled leachate outflow pipe located in the instrumented shed at the base of the dump (Fig. 1). A systematic set of simulations was run every  $5^{\circ}\text{C}$  at temperatures below and above the equilibrium temperature fixed at  $25^{\circ}\text{C}$  for the purposes of numerical modeling (corresponding to the field value of  $12^{\circ}\text{C}$ , Table 1). These simulations were made twice using the properties of dry and wet till covers. In this study, the emphasis was placed on the results for the minimum and maximum atmospheric temperatures of 5 and  $36^{\circ}\text{C}$ , respectively (corresponding to field values of  $-8$  and  $23^{\circ}\text{C}$ , respectively; Table 1). Only the dry till cover case is discussed here because, after the calibration process, the dry and wet till cover cases produced very similar results. Complementary simulations were also performed to investigate (i) the effect of high and low barometric pressures at  $36^{\circ}\text{C}$  for the dry till, (ii) what would happen if there were no pipe, and (iii) the impact of not having a till cover on the dump, in the last two cases at 5 and  $36^{\circ}\text{C}$  for dry and wet till covers.

Table 1. Temperature and pressure conditions with corresponding pneumatic potentials. The top of the dump is at an elevation of 1348 m and the pipe at the base of the dump is at 1287 m.

Imposed conditions	Min. atmospheric temperature	"Mean" dump temperature	Max. atmospheric temperature
Real temperature, °C	−8	12	23
Model temperature value, °C	5	25	36
Pressure at dump top, Pa	85,862	86,821	87,300
Pressure at pipe, Pa	86,498	87,415	87,869
Mean dump gas density, kg m <sup>−3</sup>	0.991	1.002	1.008
Mean atmospheric air density, kg m <sup>−3</sup>	1.062	1.002	0.972
Pneumatic potential at dump top, Pa†	85,862	86,821	87,300
Pneumatic potential at pipe, Pa†	85,905	86,821	87,266
Potential difference (top to pipe), Pa	−43	0	34
Dump gas general flow direction	upward	no flow	downward

† Pneumatic potentials ( $\Psi$ ) are calculated within the dump for conditions corresponding to the dump mean gas density at the internal dump temperature (25°C) and gas pressure (using Eq. [2]). The following relationships apply for the three atmospheric temperatures shown for which distinct barometric pressures  $p$  at elevation  $z$  lead to different mean dump gas densities (reference elevation at dump top):

at 5°C:  $\Psi = p + 9.7209(z - 1348)$

at 25°C:  $\Psi = p + 9.8296(z - 1348)$

at 36°C:  $\Psi = p + 9.8838(z - 1348)$

## Numerical Model Conditions

Numerical modeling of gas flow related to AMD production in waste rock dumps or coal spoils is almost always performed on two-dimensional vertical sections, as is also done for the modeling of heap leaching that involves very similar processes (Cathles and Schlitt, 1980; Jaynes et al., 1984; Pantelis and Ritchie, 1992; Kuo and Ritchie, 1999; Lefebvre et al., 2001b; Fala et al., 2005; Linklater et al., 2005; Molson et al., 2005). Such models allow the representation of gas convection due to composition or temperature changes in the dump. Such convection has a strong vertical component, thus requiring the representation of vertical gas movements, but does not significantly change laterally, thus not requiring three-dimensional models. Figure 1 shows the location of Section 0+525, which was used as a basis for the two-dimensional

vertical numerical grid of the No. 1 Shaft waste dump. This section was selected because it is representative of the central part of the dump and is surrounded by monitoring boreholes and the weather station. Because the dump has a wide central part, gas flow should be predominantly from the wide slope to the top surface and could thus be approximated as two dimensional. A two-dimensional vertical section grid should thus lead to representative simulated general gas flow patterns in the dump. Furthermore, because TOUGH2 allows the specification of a "width" to grid elements transverse to the vertical two-dimensional section, the numerical grid used for simulations actually represents a three-dimensional model that is a single element wide rather than a two-dimensional model with unit width. The equivalent width of the model grid cells was selected so that the numerical model had the same volume as the waste rock pile and thus also the same gas-filled pore volume. This configuration allowed the numerical model to represent the entire gas flow rate through the waste rock pile, as well as gas flow through the drainage pipe.

Figure 2 summarizes the main features of the numerical grid and the distribution of materials. The grid represents the slopes at the surface of the dump as well as its base, which is inclined 8° relative to the horizontal. All grid elements are vertically 1 m thick, but their lengths range from 2.5 to 10.0 m to allow a better representation of the different slopes. The horizontal transverse width of grid elements is 350 m to obtain a numerical model with a volume equivalent to the No. 1 Shaft dump. The grid has a total of 889 elements, of which 53 are "non-active". In TOUGH2 (Pruess, 1991), non-active elements have fixed conditions, and they are used to impose fixed internal or boundary conditions. In the model developed in this study, non-active elements served to impose atmospheric conditions at the dump surface, and one element is non-active to impose atmospheric conditions at the partially gas-filled drainage pipe.

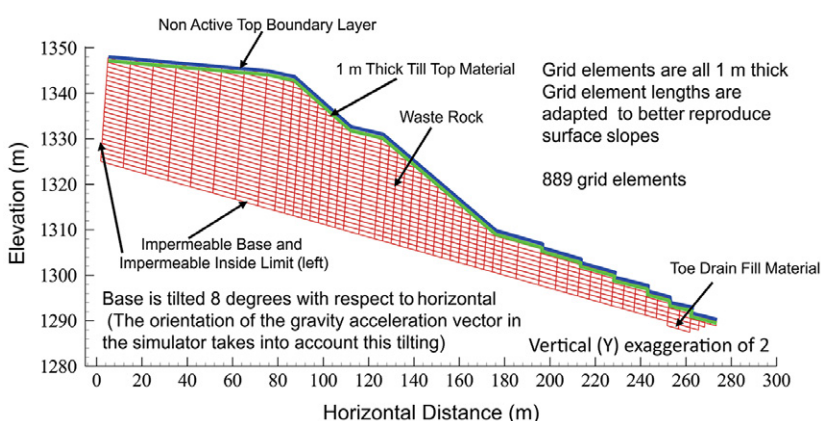


Fig. 2. Boundary conditions and material distribution in the numerical grid.

The drainage pipe is located within the toe drain fill material at the outside base of the dump, and monitoring done in the pipe included measurements of gas velocity in the pipe (in or out), gas temperature, and gas composition. TOUGH2 allows the assignment of cross-sectional areas between grid elements, whether active or non-active. The area of the non-active element representing the pipe in contact with an active drain element was assigned a value of 0.1257 m<sup>2</sup>, which represents the actual flow area of the pipe. Gas flow through the pipe (in or out) occurs in the model due to the difference in pneumatic potential between the active drain element and the non-active pipe element maintained at atmospheric pressure. Because the numerical model represents the physics, material



properties, waste rock pore volume, and geometry as under field conditions, the simulated gas flow rate through the pipe does not require any normalization or scaling. The numerical model verification and calibration can thus be done by direct comparison of observed and simulated gas velocities through the pipe.

Figure 2 also shows the distribution of materials and boundary conditions assigned to the numerical grid. At the surface of the dump, two single layers of 1-m-thick elements were used to represent non-active (fixed) boundary conditions and the underlying till cover, respectively. Almost all of the dump interior was assigned to be waste rock material, except the high-permeability fill material in the toe drain at the outer base of the dump. The pipe used to sample leachate and through which gas flows is within this drain material and it is a non-active element to which atmospheric conditions were assigned. Because the waste rock rests on low-permeability bedrock, the inside limit (left) and base of the dump were assumed impermeable and thus specified as no-flux boundaries. Surface non-active elements were assigned atmospheric temperature and pressure conditions. These non-active elements were specified as having the same properties as waste rock in order not to artificially increase the thickness of the low-permeability till cover elements. Atmospheric temperature was uniformly assigned to non-active boundary elements, including the dump surface and pipe. However, atmospheric pressure had to be applied with a value decreasing with elevation, in accordance with the atmospheric air density, to represent a stagnant hydrostatic gas column. Otherwise, the applied pressure could induce gas flow in the dump. Even though non-active surface elements were assigned an atmospheric temperature different from the internal dump temperature, no heat transfer was considered; that means that temperatures were assigned and fixed in the model and that fluids (gas in this case) take the temperature of the grid cell in which they are present. However, imposing atmospheric temperatures to non-active surface elements provided inflowing air densities and viscosities representative of the atmospheric temperature.

Monitoring data from the weather station showed that the temperature varies by about 30°C, from -8 to 23°C, and barometric pressure ranges from 85,000 to 88,000 Pa, with a mean of about 86,700 Pa (raw uncorrected pressures at the elevation of the weather station located on the dump). When the atmospheric temperature is around 10 to 12°C, monitoring data also showed no gas flow through the pipe, so no gas exchange between the dump and atmosphere (Fig. 3, further discussed below). This equilibrium temperature thus represents the effective mean global gas temperature in the dump, considering that the dump gas phase has a molar mass equivalent to the atmospheric air. The magnitude of gas exchanges between the dump and atmosphere should depend on the difference of the atmospheric temperature from the equilibrium temperature. To simulate these gas exchanges, the numerical model thus has to represent the full range of 30°C temperature variations. However, the equation of state in TOUGH AMD cannot represent temperatures <0°C. Despite this limitation,

because it is the difference in temperature relative to the equilibrium that controls gas exchanges, the model uses an equilibrium temperature of 25°C, which allows the model to represent  $\pm 15^\circ\text{C}$  changes without reaching negative values.

Table 1 summarizes the range of atmospheric temperatures and corresponding atmospheric pressures imposed as boundary conditions based on the observed variations at the site. Base simulations under hydrostatic conditions, without gas flow in the dump, were performed at 25°C, the model temperature assigned to the dump. These simulations provided the initial conditions used for simulations performed at other temperatures. This study highlights the results obtained for the two “extreme” temperature cases at 5 and 36°C, representing the normal range of variation for atmospheric temperature at the site. Intermediate simulations were performed every 5°C between 5 and 45°C to obtain a complete view of the simulated conditions. Table 1 also shows the atmospheric pressures corresponding to the imposed atmospheric temperatures. These different atmospheric pressures strictly depend on the changes in temperature that induce different gas densities, thus leading to significant changes in barometric pressure due to the high elevation of the site. Table 1 shows pressure values imposed at the top of the dump and at the pipe located near its base. The barometric pressure imposed on the dump surface varies approximately linearly with elevation between these two values. However, the numerical model accounts for the not strictly linear changes in barometric pressure with elevation on the boundary elements.

Table 1 presents calculations of the potential differences resulting from gas density differences between the atmosphere and the dump gas phase due to their different temperatures, considering the total thickness of the dump. Table 1 shows these pneumatic potential differences to indicate what is driving the flow; it is not showing values imposed a priori to trigger the flow in the numerical model. Rather, the boundary condition imposed on the dump surface is a “hydrostatic” atmospheric pressure profile with elevation corresponding to the atmospheric temperature. Such a “hydrostatic” pressure profile was obtained by a prior numerical simulation that led to no vertical fluxes of gas in the atmosphere or in the dump if it is at the same temperature as the atmosphere. This ensures that boundary conditions do not induce gas flow artifacts. When the atmosphere is not at the same temperature as the dump, the pneumatic potential difference across the dump surface is then a consequence of the difference in gas-phase density between the atmospheric air and the gas phase in the dump (see the definition of the pneumatic potential in Eq. [2]). These gradients in pneumatic potential then lead to gas flow through the dump surface and gas circulation in the dump. Darcy’s law then imposes that such flow induces pneumatic potential losses in the direction of flow, either through the till cover or through the waste rock. The observation wells at the study site provided indications of these gradients in potential, and they were used to qualitatively validate the model, but the installations were not adequate to provide quantitative indications such as those used by Lefebvre et al. (2012)

for a site in Germany where differential pressures between the atmosphere and waste rock were measured right across the dump cover. Below we illustrate the gas flow behavior represented by the use of these model conditions as well as the material properties.

Table 2 summarizes the material properties derived from the available data on the No. 1 Shaft waste rock dump (details in Lahmira and Lefebvre, 2008). Till properties were determined on the basis of available laboratory and field measurements. Using the available grain-size distributions, waste rock properties were estimated by comparison of its grain size distribution to analog waste rock whose properties were measured in the laboratory. The median diameters ( $d_{50}$ ) for the available grain-size distributions are 4, 3.5, and 5 mm, respectively. Representative soil moistures of the till for wet and dry conditions were based on measured soil moisture profiles on the No. 1 Shaft dump. A representative waste rock soil moisture was obtained by assuming capillary equilibrium with the till cover.

### Model Calibration and Validation

Material properties were modified by trial and error from their initial estimate to calibrate and validate the model. The following criteria were used to determine if the model was representative and appropriately calibrated: (i) the direction (in or out) and magnitude of pipe gas flow as a function of atmospheric temperature; (ii) the gas pressure gradients generated between the dump and the atmosphere compared with those measured at observation wells; (iii) the gas flow patterns compared with patterns inferred based on gas pressure gradients and gas composition measured in observation wells; and (iv) the time for the system to reach steady state, as monitoring data showed that pipe gas velocities and directions quickly follow changes in atmospheric temperature with a short lag time (generally <30 min). Lahmira and Lefebvre (2008) further described the observations obtained from the No. 1 Shaft dump monitoring system that formed the basis of the model calibration criteria.

The effective air permeability is the property that had to be modified the most to calibrate the model. The value of the effective air permeability had to be significantly increased, to at least  $5 \times 10^{-12} \text{ m}^2$  for the till cover and  $5 \times 10^{-9} \text{ m}^2$  for the waste rock, to reproduce

the observed gas flow behavior of the dump, especially the magnitude of the pipe gas flow velocity. These values represent increases of more than one and two orders of magnitude, respectively, for the dry and wet till covers. For the waste rock, the increase in effective air permeability above the initial estimate is more than two orders of magnitude. Such large increases above estimated values for the till cover, especially under wet conditions, were thought to indicate that the threshold effective air permeability required to calibrate the model is more likely related to local variability in the cover (fissures, grain size variations, compaction, or thickness variations, etc.) than a poor initial estimate of the properties of a “sound” till cover. The presence of such local variability is perhaps indicated by the observed localized melting of snow over the dump surface that could be due to preferential warm gas exiting from the dump (Phillip et al., 2009). Similarly, the large increase in effective air permeability for the waste rock above the initial estimate could reflect the heterogeneity of the dump and the presence of preferential gas flow paths through coarse, high-permeability material. Such internal heterogeneities and the variability in the waste-rock grain size were indicated by an electrical resistivity survey of the dump and further drilling (Phillip et al., 2009). Lahmira et al. (2007) showed through numerical simulations that heterogeneous waste rock leads to preferential water flow through fine-grained material, leaving coarse permeable material available for gas flow. This indicates that local measurements may provide a non-representative indication of the bulk hydraulic properties of systems as heterogeneous as waste rock dumps and even carefully installed cover layers.

It is important to point out that the simulations used “equivalent” homogeneous material properties to represent the till cover and waste rock, which are probably heterogeneous. These equivalent properties, which differ from the initially estimated properties, do not imply that these initial estimates were necessarily wrong or that the cover is generally performing more poorly than what laboratory and field measurements would tend to show. Instead, these equivalent properties are thought to be strongly influenced by the presence of preferential flow paths in the waste rock and local variability of the till cover. Furthermore, the properties of waste rock and till cover are not independent, so other combinations of these properties could as well have led to model calibration. The presence of preferential

gas flow paths through the waste could also have an effect on the equivalent cover permeability. The preferential flow paths would allow high pneumatic potential gas to be in contact with localized points of the cover. If some of those points were more permeable than the bulk of the cover, significant gas flow could result. When the model is calibrated by adjusting the equivalent homogeneous bulk properties of the waste rock and cover, these localized effects cannot be considered. The implication of this discussion is that the calibration of the

Table 2. Material properties used in the numerical model.

Property	Dry till	Wet till	Waste rock	Drain and pipe†
Total porosity	0.295	0.295	0.33	0.45
Residual water saturation	0.80	0.950	0.35	0.45
Hydraulic conductivity, $\text{m s}^{-1}$	$5.00 \times 10^{-6}$	$5.00 \times 10^{-6}$	$1.00 \times 10^{-4}$	$1.00 \times 10^{-3}$
Estimated effective air permeability, $\text{m}^2$	$1.46 \times 10^{-13}$	$9.41 \times 10^{-15}$	$9.34 \times 10^{-12}$	$1.02 \times 10^{-10}$
Model effective air permeability, $\text{m}^2$	$5.10 \times 10^{-12}$	$5.10 \times 10^{-12}$	$5.02 \times 10^{-9}$	$5.02 \times 10^{-5}$
van Genuchten $\alpha$ parameter, $\text{Pa}^{-1}$	0.000008	0.000008	0.00085	
van Genuchten $m$ parameter	0.55	0.55	0.3	
van Genuchten $n$ parameter	2.22	2.22	1.43	

† Material filling the drainage ditch in which the pipe is installed.



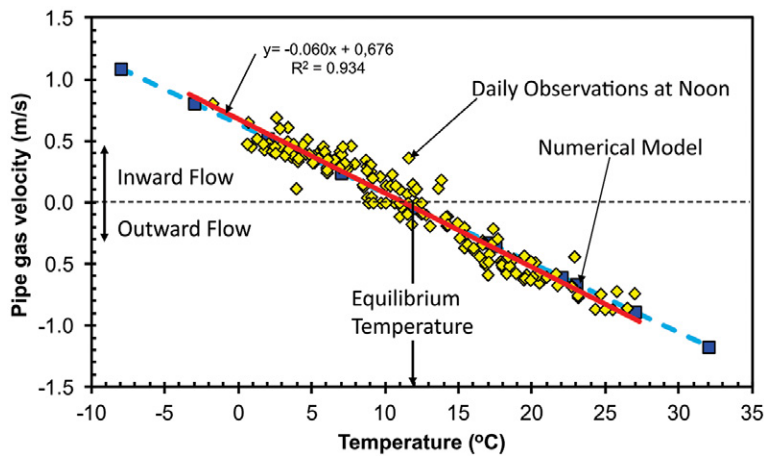


Fig. 3. Comparison of simulated and measured gas velocities in the partially gas-filled leachate drainage pipe at the toe of the dump (beginning of April–end of October 2007), showing all points from modeling results. Simulation results (blue squares) are shown at temperatures of the actual system corresponding to simulation temperatures. Observations shown (yellow diamonds) are selected daily values measured at noon. The red line is the linear regression of observations. The dashed blue line linearly links simulation results under final steady-state conditions.

till cover permeability should not be taken to represent a “correction” to the original estimates. Under the assumption that the effective air permeability required to calibrate the model did not reflect an intact till cover but the potential effect of preferential paths through the cover, the same effective air permeability was used for both dry and wet till covers. If local variability controls the overall cover permeability, it would not be of interest to investigate values even higher than the “threshold” required for calibrating the model. Under such conditions, we do not discuss differences between dry and wet till simulations because these led to similar results.

Figure 3 compares the measured pipe gas velocities as a function of atmospheric temperature with the numerical simulation results. Positive pipe gas velocities correspond to gas flow into the pipe, whereas negative values represent gas flow out of the pipe. Simulations were performed for a dry till cover at 5°C intervals above and below the equilibrium temperature. Simulation results (blue squares) are shown at temperatures of the actual system corresponding to simulation temperatures (Table 1). The observations shown (yellow diamonds) are selected daily values measured at noon. The red line is the linear regression of observations. The dashed blue line linearly links the simulation results under final steady-state conditions.

Pipe gas velocities provide the best indication of the importance and direction of gas flow in the dump. At atmospheric temperatures equal to the equilibrium temperature of 10 to 12°C corresponding to the mean waste rock temperature, there is no gas flow through the pipe, whereas pipe gas velocity is positive (into the pipe) at atmospheric temperatures lower than the equilibrium and negative (out of the pipe) at atmospheric

temperatures above the equilibrium. Pipe gas velocity is strongly negatively correlated to the atmospheric temperature ( $R^2 = 0.93$ ). Simulated pipe gas velocities very closely followed observations, showing that the model is properly calibrated. The model is also validated by comparison with other monitoring observations that are consistent with the simulation results (Lahmira and Lefebvre, 2008). On that basis, a conceptual gas flow model was developed that guided the development of the numerical model used to simulate dump gas flow (Lahmira and Lefebvre, 2008). Generally, variations in gas composition and differential pressures measured in monitoring boreholes, as well as the temperature profiles, were found to be consistent with the simulated conditions and gas-flow patterns. However, longer term pipe gas velocity data through the winter months seem to indicate that there may be more moderate changes in velocity with changes in temperature in the colder periods (Phillip et al., 2009). This may perhaps be due to the partly sealing effect of the snow cover or till freezing, at least in the gas entry areas, because melted snow was observed on the presumed preferential gas exit areas (Phillip et al., 2009). This process was not considered in the numerical simulations done in this study.

## Simulated Gas Flow Behavior

Table 1 lists the pneumatic potential values calculated at the dump top surface and the pipe for the minimum, mean (equilibrium), and maximum atmospheric temperatures encountered at the site. The table also presents the mean dump gas and atmospheric air densities at these temperatures. The differences in density between dump gas and atmospheric air indicates that dump gas flow should generally be upward and downward at low and high atmospheric temperatures, respectively. The magnitude of this flow will depend on the pneumatic potential differences between the top of the dump and the pipe. The direction of dump gas flow is also shown by the fact that the pneumatic potential is lower than at the pipe under low atmospheric temperature and higher at high temperature.

## Gas Flow in the Dump at Low and High Temperatures

For simulations at atmospheric temperatures of 5 and 36°C, Fig. 4 and 5, respectively, show calculated pneumatic potentials corresponding to the simulated conditions with a color scale. Each figure shows the conditions for three simulated cases: the base case with a dry till cover and a pipe, the case with a dry till cover and no pipe, and the case without a till cover but with a pipe. The simulated high and low barometric pressure cases are not illustrated because these results were very similar to the base case but with shifted absolute pneumatic potential values. Figures 4 and 5 also show streamlines indicating gas flow paths within the dump. Arrows along these streamlines indicate

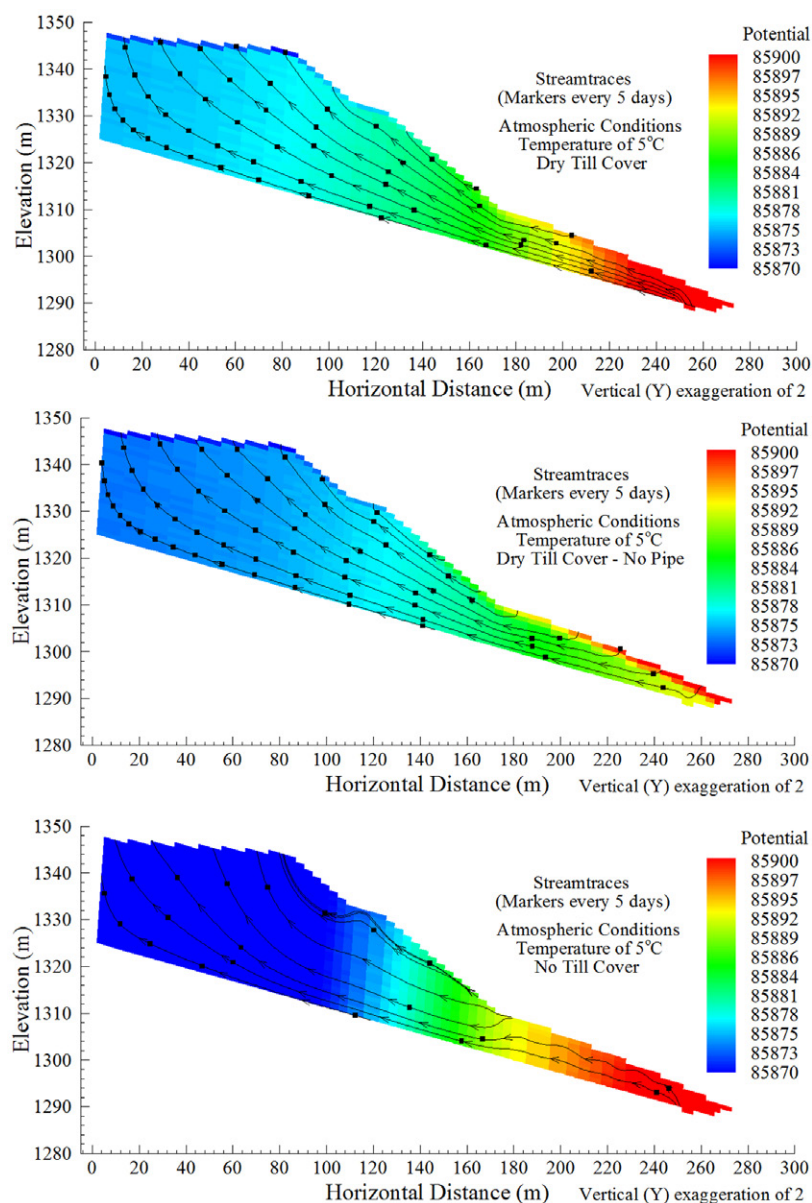


Fig. 4. Pneumatic potential (Pa) and stream traces at 5°C for the dry till cover with the pipe (top), without a pipe (middle), and with a pipe but without a till cover (bottom).

the gas flow direction, whereas black squares are time markers whose spacing indicates a 5-d flow duration.

The top graphs of Fig. 4 and 5 represent simulated conditions for the base case at 5 and 36°C, respectively. Although dump gas flows in opposite directions at these different atmospheric temperatures, the gas-flow patterns have common features. First, most of the gas exchanges between the dump and atmosphere occur through the pipe (and toe drain) and the top surface of the dump. This is indicated by the fact that a vast majority of the streamlines extend from the pipe to the top surface of the dump. The area of the pipe and toe drain within the dump has a potential similar to that of the dump surface boundary under atmospheric conditions. However, even though gas flow occurs through the till cover, its permeability

is much lower than that of the waste rock, so there is a large potential difference between the uppermost part of the dump and the boundary at the top dump surface as gas flows through the cover (shown by the contrast in color representing potential magnitude). This feature is also apparent on the graphs of pneumatic potential vs. elevation shown in Fig. 6. There are limited exchanges through the till cover along the dump slope, as indicated by the few streamlines originating from the slope. On that slope, gas is exchanged in different directions through the till in the upper and lower parts of the dump slope. The general patterns of gas flow indicated by the numerical model are supported by field observations of differential pressure across the till cover and the gas composition in the dump, discussed further below (Fig. 7).

Gas velocities are low in the interior and top portion of the dump, become higher in the center of the slope, and are highest in the lower thin portion of the dump, as indicated by the spacing of streamline time markers in Fig. 4 and 5 (farther apart markers indicate faster gas flow). Because slow flow occurs through the till cover, there is about the same total gas flow rate from the top dump surface to the pipe located at the base of the dump. Gas velocity is thus related to the available gas flow cross-section through the dump, which is much larger in the thick upper part of the dump than in the thin lower portion near the base of the dump. Gas velocities are higher for the case at low atmospheric temperature (5°C) than at high temperature (36°C) due to the higher difference in pneumatic potential between the dump top surface and the pipe at 5°C compared with 36°C (Table 1). These differences in gas velocity between these two cases influence the total gas transit time through the dump. The transit time actually depends on the position within the dump. For the case at 5°C, if the atmospheric temperature remained constant, it would take more than a month for gas to transit through the lower part of the

dump, whereas the transit time would be <20 d through the upper portion of the dump closer to the slope. In the case of gas transiting across the dump slope, its transit time would be <10 to 15 d. Because gas flow is slower for the 36°C case, the total transit time would take >2 mo in the lower part of the dump and on the order of 40 d in the upper portion of the dump close to the slope.

## Role of the Toe Drain and Pipe and the Till Cover

The middle graphs of Fig. 4 and 5 show potentials and streamlines for the simulation case without a pipe at 5 and 36°C atmospheric temperatures, respectively. Compared with the base case, the absence of a pipe results in the same general flow direction and quite similar gas flow patterns through the dump. Without a pipe,



the main difference compared with the base case is that gas has to flow through the till cover in the lower part of the dump. There is an important potential loss as gas flows through the till (shown by the contrast in color related to potential magnitude). This is also apparent in Fig. 6. Gas velocity is decreased in the lower part of the dump compared with the base case due to more restricted gas exchanges between the dump and atmosphere in the absence of the pipe. The results for simulations without a pipe should be compared only with the base case because they are not meant to represent what would actually occur without a pipe but rather to show the role of the pipe under the conditions presently prevailing in the dump.

The lower graphs of Fig. 4 and 5 show potentials and streamlines for the simulation case without a till cover at atmospheric temperatures of 5 and 36°C, respectively. Compared with the base case, the absence of a till cover leads to much faster gas flow in the dump. Because there is no till cover, in this case there is no potential loss across the dump surface. This leads to increased gas entry in the dump through the slope as well as in the pipe. However, gas entry through the pipe is relatively less important than gas entry through the slope. This is indicated by the fact that fewer streamlines are transiting through the pipe than what occurred for the base case. Gas velocities are higher through the dump than in the base case, except through the lower part of the dump. Again, the results of the simulations without a cover should be compared only with the base case because they are not meant to represent what would actually occur without a cover but rather elucidate the role of the cover under the present conditions of the dump.

## Simulated Pneumatic Potential

Figure 6 presents graphs of pneumatic potential vs. elevation in the dump for simulated conditions prevailing after 12 h, i.e., near steady state. Under these conditions, there is equilibrium between the imposed atmospheric temperature and pressure on the dump and gas flow within the dump. The three main simulation cases are presented: base case, no pipe, and no cover. Table 1 shows that imposed atmospheric conditions lead to pneumatic potential gradients between the top surface of the dump and the pipe. In Fig. 6, the potentials related to boundary atmospheric conditions appear as linear trends spanning the entire dump elevation range (indicated by red lines). For a given atmospheric temperature, these trends are the same for all three simulation cases because the boundary conditions are identical for these cases. These linear, vertical pneumatic potential gradients at the dump surface control the direction of dump gas flow. For low atmospheric temperature

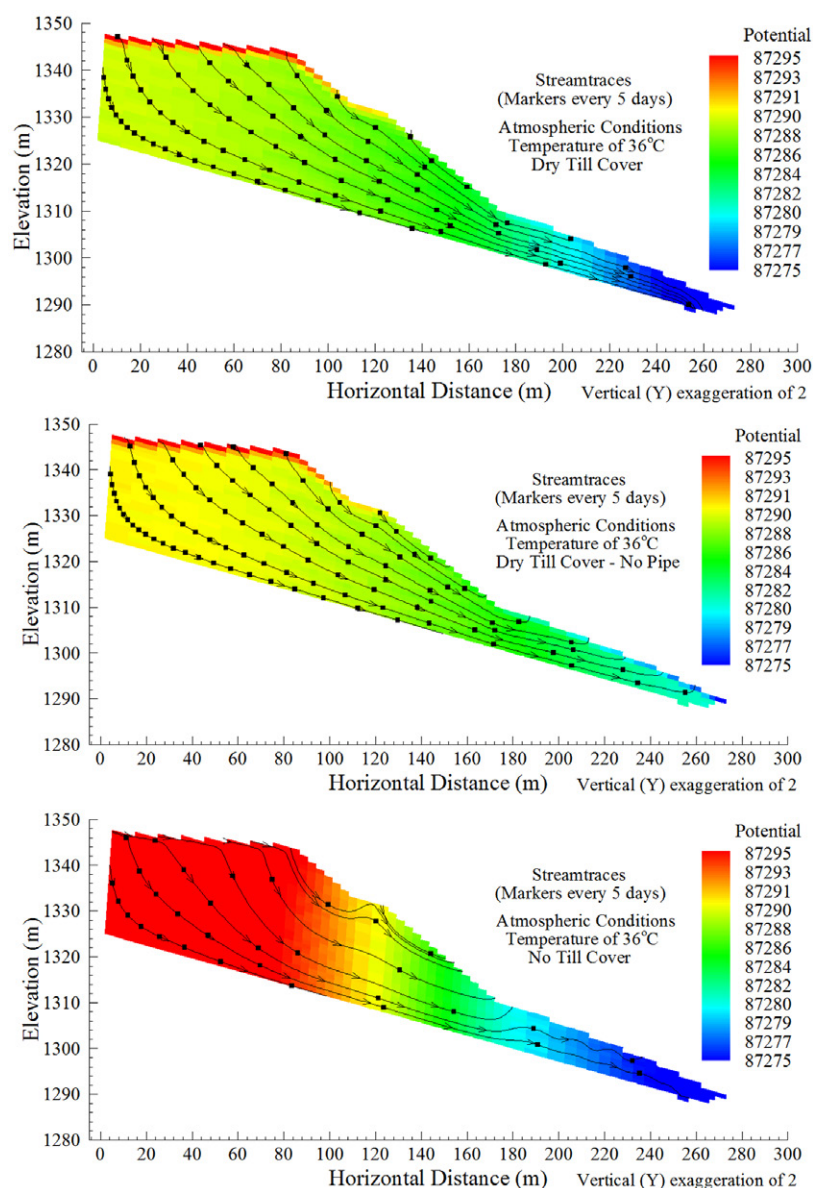


Fig. 5. Pneumatic potential (Pa) and stream traces at 36°C for the dry till cover with the pipe (top), without a pipe (middle), and with a pipe but without a till cover (bottom).

(5°C), the imposed boundary pneumatic potentials decrease with elevation, which leads to upward gas flow, whereas at high atmospheric temperature (36°C), the imposed potentials increase with elevation, which imposes downward gas flow.

The top graphs of Fig. 6 correspond to the base case. Because there is a direct link between the dump and the atmosphere provided by the pipe and toe drain, the lower part of the dump gas has the same pneumatic potential as the atmosphere. As gas flows through the dump, there is a pneumatic potential loss along the flow direction, upward for the 5°C case and downward for the 36°C case. This loss is more important (higher gradient) in the lower part of dump where the flow cross-section is restricted, whereas very little potential loss occurs in the upper thick part of the dump.



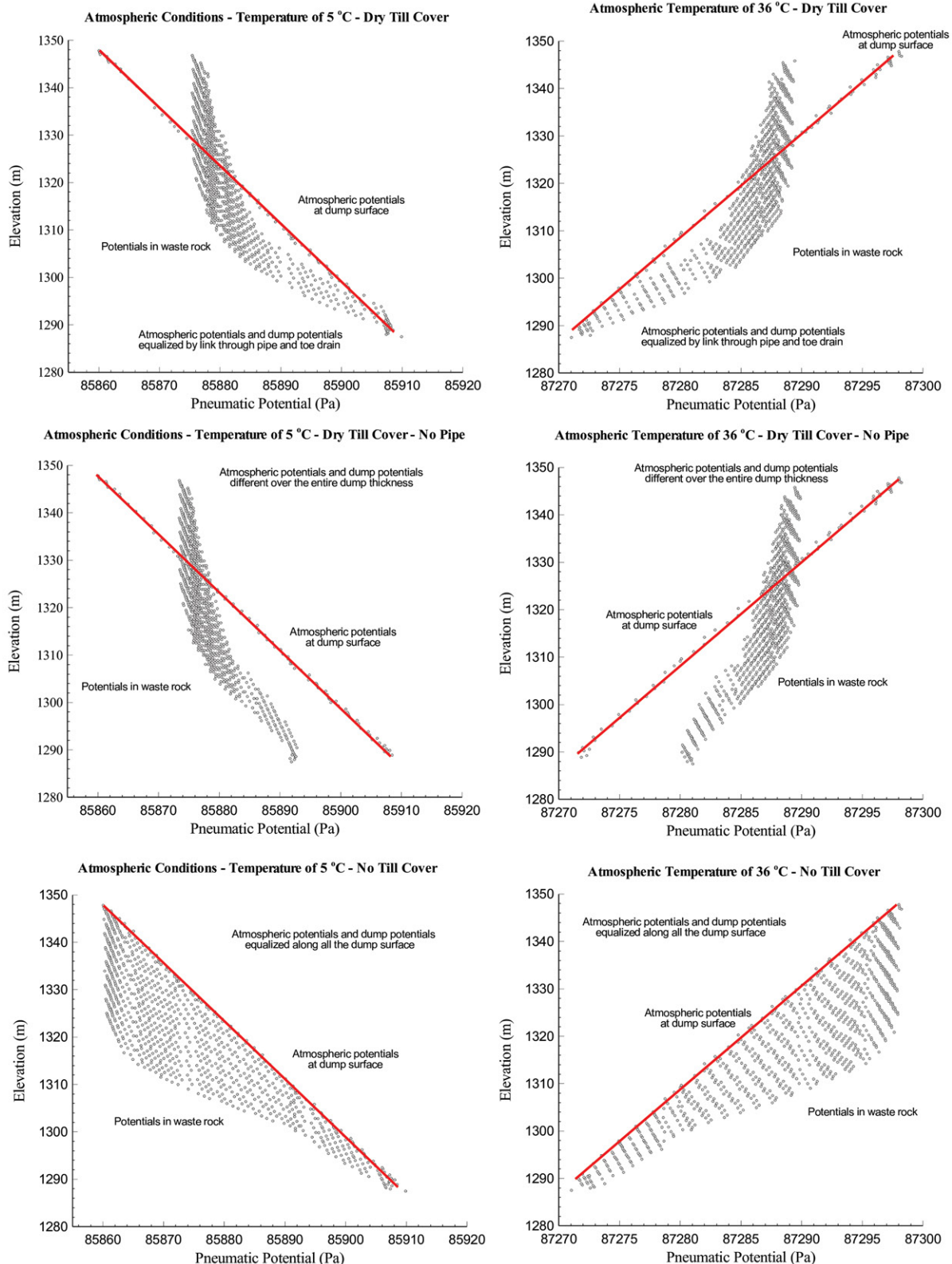


Fig. 6. Vertical distribution of pneumatic potentials at 5°C (left) and 36°C (right) for the dry till cover with the pipe (top), without a pipe (middle), and without a till cover (bottom). The dots represent the potentials calculated for each grid element. The line superposed on the dots represents the potentials corresponding to atmospheric conditions imposed at the dump surface. There will be a tendency for horizontal flow to occur between the atmosphere and the dump if the atmospheric potential is different from that of the dump gas. There will be a tendency for vertical flow (upward or downward) in the dump if there is a vertical gradient in dump gas potential.

The dump gas pneumatic potentials cross the atmospheric values at an elevation of about 1320 m. Above and below this elevation, the difference in potential between the atmosphere and dump gas leads to limited gas exchange across the till cover due to its low effective air permeability. There is a large difference in potential between the atmosphere and dump gas at the top of the dump that corresponds to the potential loss occurring while gas flows through the till cover at the top surface of the dump.

The central graphs of Fig. 6 show the trends in pneumatic potential with elevation for the cases without a pipe. The main difference relative to the base case is that the upper and lower ends of the dump are at different pneumatic potentials than the atmosphere. Under these conditions, there are thus large potential losses as gas flows through the till cover at the base and upper portion of the dump slope, to either enter or exit the dump.

The lower graphs of Fig. 6 show the conditions for the cases without a till cover. This time the main difference compared with the base case is that dump gas potentials are the same as atmospheric potentials along the entire slope of the dump. In the absence of a cover, there is no potential loss as gas flows through the dump surface, which leads to an overall larger dump gas potential gradient from the base to the top of the dump. This induces larger overall gas flows through the dump and more important gas exchanges between the dump and atmosphere without a till cover.

## Gas Flow Conceptual Model

Table 3 summarizes the monitored conditions in observation boreholes, whose locations are shown in Fig. 1 and projected positions on the numerical grid are indicated on Fig. 7. The conditions compiled in Table 3 indicate the gas flow conditions prevailing in the No. 1 Shaft dump. On this basis, a gas flow conceptual model was developed that guided the development of the numerical model used to simulate dump gas flow. These conceptual models are presented so that the observations that formed the basis for their development can be compared with the numerical simulation results. Such a comparison further validates the numerical model and ties together numerous observations made on conditions prevailing in the No. 1 Shaft dump.

Observed thermal conditions are the first data compiled in Table 3. Atmospheric temperature is presented as a reference, and the values for the low, mean, and high temperatures were obtained from a sinusoidal fit to the meteorological temperature data. Values of borehole-monitored parameters are representative of these different atmospheric temperature ranges. The borehole temperatures listed in Table 3 are derived from measured monthly profiles that are affected by cyclic yearly air temperature variations. Boreholes BH-1A and BH-1B are the only ones deeper than the range affected by cyclic yearly air temperature variations (about 10 m). Below about the 5-m depth, temperatures ranged from about 8 to 16°C, with average values between about 10 to 14°C (Fig. 3). Table 3 also

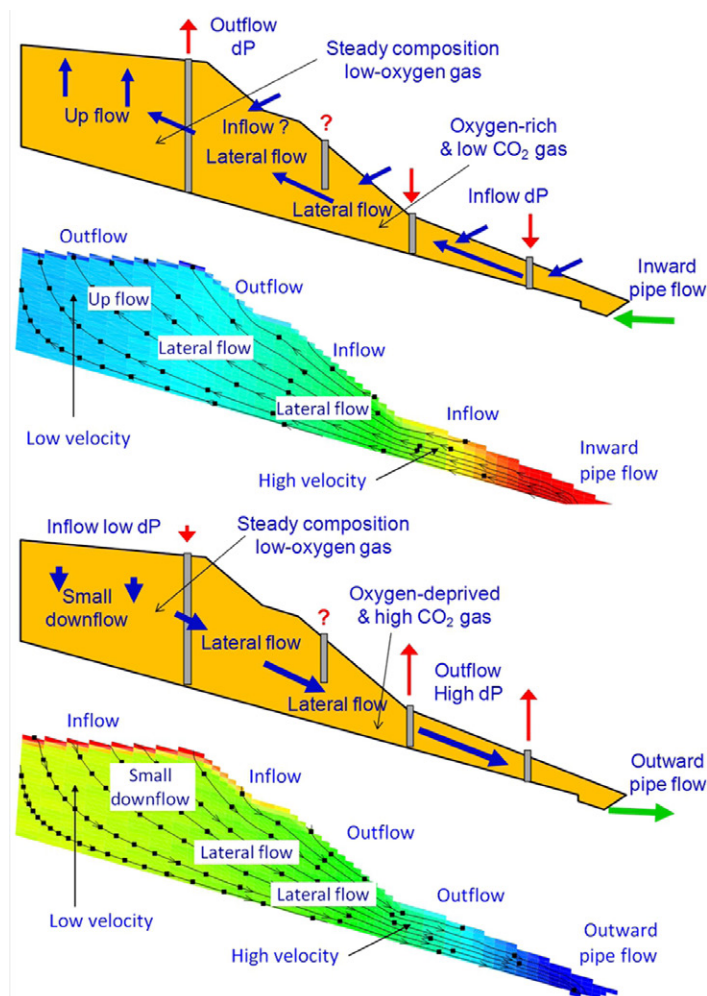


Fig. 7. Comparison of the conceptual model of gas flow with numerical results for low (top) and high (bottom) atmospheric temperatures; dP is differential gas pressure.

compiles the gas compositions observed in the boreholes, which were found to be quite variable seasonally. Boreholes BH-1A and BH-1B have more stable gas compositions with low O<sub>2</sub> (1–5%) and high CO<sub>2</sub> (4–6%). At low temperatures, O<sub>2</sub> concentrations are slightly higher, whereas CO<sub>2</sub> concentrations are lower. Borehole BH-2A has very low O<sub>2</sub> (1%) and very high CO<sub>2</sub> (10%) concentrations. This borehole may be isolated from the main gas flow system. Boreholes BH-2B, BH-3A, and BH-3B have widely varying seasonal gas concentrations, with high O<sub>2</sub> (can even be atmospheric) and low CO<sub>2</sub> under low air temperatures and almost no O<sub>2</sub> and high CO<sub>2</sub> (which can exceed 12%) under high air temperatures. Representative values of gas densities calculated for the temperatures and gas composition found in the boreholes are compared with atmospheric air densities. Finally, Table 3 compiles the differential gas pressures (dP) measured in the boreholes, which indicate vertical gas flow tendencies. The measurements made when the borehole gas was sampled are those shown in the table. The convention used for dP measurements is atmospheric pressure minus borehole pressure. Positive values of dP thus indicate downward flow tendencies, whereas negative values show upward flow tendencies.

Table 3. Summary of monitored conditions in boreholes (conditions observed as of December 2007, when the numerical model was developed).

Borehole	Temperature ( <i>T</i> )	O <sub>2</sub>	CO <sub>2</sub>	Differential pressure flow direction	Gas density
	°C	—————%—————			kg m <sup>-3</sup>
Atmosphere					
Low <i>T</i>	−8				1.137
Mean <i>T</i>	7.5				1.071
High <i>T</i>	23				1.008
BH-1A					
Low <i>T</i>	10	2.3	4.4	up fast at low <i>T</i>	1.060
Mean <i>T</i>	13.7	1.2	5.1	mostly up	1.045
High <i>T</i>	16	1.1	5.7	down >> 20°C	1.035
BH-1B					
Low <i>T</i>	10	2.5	4.5	up fast at low <i>T</i>	1.060
Mean <i>T</i>	13.7	3.2	4.5	mostly up	1.045
High <i>T</i>	16	4.8	4.5	down >> 20°C	1.035
BH-2A					
Low <i>T</i>	7				
Mean <i>T</i>	10	1.3	10		
High <i>T</i>	13				
BH-2B					
Low <i>T</i>	7	10.2	1.9	down when cold	1.057
Mean <i>T</i>	10	3.9	4.5		1.050
High <i>T</i>	13	0.2	6.7	up when hot	1.040
BH-3A					
Low <i>T</i>	8	11.7	2.1	down when cold	
Mean <i>T</i>	11	7.7	4.4		
High <i>T</i>	14	0.3	8.6	up when hot	
BH-3B					
Low <i>T</i>	11	8.5	2.7	down when cold	1.043
Mean <i>T</i>	13	5.3	4.3		1.039
High <i>T</i>	16	1.2	6.25	up when hot	1.032
Pipe					
Low <i>T</i>				flow in	
Mean <i>T</i>					
High <i>T</i>		1–2	5.6–7	flow out	

The data compiled indicate that both the sign and magnitude of dP vary seasonally. In boreholes at the top of the dump (BH-1A and BH-1B), dP indicates mostly upward gas flow, except when the air temperature is high (above about 20°C). The magnitude of dP is relatively low for these boreholes. The reverse behavior in dP is seen in other boreholes lower down in the dump: dP indicates downward flow under cold conditions and upward flow under warm conditions, with relatively clear changes in direction with the seasons at threshold values in the range of 12 to 13°C. Figure 7 compares numerical simulations for the low- and high-temperature base cases with the conceptual model of gas flow in the No. 1 Shaft dump

based on monitoring data. The conceptual model was based on the observed differential pressures and gas compositions in observation wells and from pipe velocities (Table 3). Both at low and high atmospheric temperature, the assumptions of the conceptual model are supported by the numerical results.

At low atmospheric temperature, air enters the pipe, then gas flows laterally at high velocity in the lower part of the dump and then slowly upward in the upper part of the dump. This generally upward flow tendency was assumed in the conceptual model on the basis of air entry in the pipe and differential pressures measured at the top of the dump indicating upward flow (Table 3). Lateral gas flow in the lower and central part of the dump was supported by the temperature profiles measured in observation wells that indicated heat production, thus O<sub>2</sub> supply and gas flow, throughout the entire thickness of the dump. The large air inflow in the lower part of the dump was also supported by high O<sub>2</sub> concentrations observed in that part of the dump (Table 3). Lower gas velocities in the upper part of the dump were assumed on the basis of the dump geometry and the low O<sub>2</sub> concentrations observed in the upper part of the dump. The model also supports the tendency for gas to flow downward through the till cover in the lower part of the dump and flow upward in the upper part of the dump (Table 3). These flow tendencies were deduced from pressure gradients observed in boreholes located in the upper and lower portions of the dump slope. The numerical model contradicts the conceptual model only with respect to gas entry through the till cover in the upper part of the slope that was assumed on the basis of gas composition. Oxygen was observed at that location in the dump, and it was thought that significant air entry occurred there to explain this O<sub>2</sub>. This could perhaps rather be explained by a local inflow of air reaching an observation well rather than as representing the general flow pattern in the dump.

At high temperature, dump gas exits through the pipe and there is rapid lateral gas flow in the lower part of the dump and slow gas flow in the upper part of the dump. This pattern was again inferred from pipe gas flow and pressure gradients observed on the top of the dump (Table 3). The strong lateral gas flow in the lower part of the dump was also indicated by the O<sub>2</sub>-depleted and CO<sub>2</sub>-rich composition of dump gas flowing through the pipe. Such a composition shows that air has not significantly entered the dump along the gas flow path and that gas comes from within the dump where O<sub>2</sub> is consumed and CO<sub>2</sub> produced. The tendency for gas entry and exit through the till cover in the lower and upper



part of the dump slope, respectively, was again based on differential pressures measured in the boreholes (Table 3). The numerical modeling results also support the assumption made that gas flux would be lower at the higher atmospheric temperatures relative to the lower ones.

These agreements between various monitoring observations with model predictions further validate the numerical model, which was shown to be calibrated on the basis of its predictions of pipe gas velocities as a function of temperature (Fig. 3). However, the model does not represent the potential effects of heterogeneities in the waste rock and till cover. Such heterogeneities could lead to preferential gas flow paths and gas stagnation zones in the dump.

## Conclusions

The numerical model developed to represent gas flow in the Sullivan Mine No. 1 Shaft waste rock dump reproduces the gas velocities observed in the drainage pipe at the base of the dump as a function of temperature and is in general agreement with monitoring observations. To calibrate the model, the effective air permeability of the till cover and waste rock had to be significantly increased from the initial estimates based on the available data. We presume that the increased permeabilities required by the model reflect the combined effects of coarse preferential flow paths in the waste rock and localized variability in the cover. There are probably other combinations of permeabilities for the till cover, waste rock, and toe drain fill material that would have allowed model calibration. Representative results obtained from the simulations support the simplifying assumptions made to develop the model, mainly that (i) the presence of  $\text{CO}_2$  in the dump gas could make its molar mass equivalent to that of atmospheric air, (ii) the mean dump temperature remains relatively constant, and (iii) water flow in the dump does not significantly alter gas flow.

The physical process causing gas flow in the dump is thermal convection due to dump gas buoyancy. The dump gas buoyancy depends on its density difference relative to atmospheric air. The difference between dump gas and atmospheric air densities depends only on their respective temperatures: the dump gas temperature remains quite constant, whereas the atmospheric temperature is variable and thus controls the gas flow direction and magnitude. The dump is assumed to maintain a relatively steady temperature of about 10 to 12°C. When the atmospheric temperature is similar to the mean dump temperature, there will be no tendency for dump gas to flow. However, when the atmospheric temperature is lower than 10 to 12°C, its density is higher than that of the dump gas, which will then tend to rise up through the atmosphere (positive buoyancy), and air will enter the pipe. On the contrary, when the atmospheric temperature is higher than 10 to 12°C, its density is lower than that of the dump gas, which will tend to sink down through the atmosphere (negative buoyancy), and dump gas will exit the pipe. Under these conditions, the dump gas will tend to be less dense

than the surrounding atmosphere in winter and denser during summer. Such a mechanism implies that gas flow is controlled by external forces, namely atmospheric temperature, rather than by the properties of its cover or waste rock, as long as these materials are permeable enough to allow buoyancy-driven gas flow to occur.

Gas flow in the dump is not significantly affected by barometric pressure changes because it does not significantly affect the relative density of dump gas and atmospheric air. The pipe and high-permeability toe drain fill material facilitate gas flow and exchanges with the atmosphere. The system was found to rapidly reach steady-state gas flow conditions, in about 15 min, even following major perturbations in atmospheric temperature and pressure. Gas flow through the pipe and till cover can rapidly provide the relatively small gas volume required to compensate for the effects of simulated atmospheric temperature and pressure changes. The natural system does not undergo such drastic changes, and the system reaches a new dynamic equilibrium related to variations in atmospheric conditions.

Most of the gas flowing through the dump enters or exits through the pipe. However, for a “cold dump” such as the one studied, there would still be similar gas flow patterns without the presence of the pipe. Similarly, although the till cover restricts gas exchanges between the dump and the atmosphere, a low-permeability cover is not required to obtain the observed gas flow behavior in such a cold dump. Actually, there would even be more gas flow without a cover and gas would similarly flow through the pipe. A perfectly sealing dump cover would not lead to the observed gas flow behavior.

The general conditions that could lead to a gas flow behavior similar to that observed at the No. 1 Shaft dump can be inferred from the characteristics of that dump and the processes that were shown to be controlling gas flow:

- A low mean internal dump temperature, within the range of yearly atmospheric temperature variations, means that dump gas and atmospheric air densities have the possibility to be similar. For example, such low dump temperatures could occur in low-reactivity dumps, moderate-permeability dumps, or covered dumps.
- The waste rock dump has to be permeable enough (waste rock and cover combined) to allow buoyancy-driven gas convection to dominate exchanges in gas flow between the dump and atmosphere.
- A relatively large dump thickness would be favorable, as this would help maintain a steady internal dump temperature by avoiding too much influence from yearly atmospheric temperature variations.
- The geometry of the dump may play a role, as an important vertical component and sloping base may favor vertical gas flow related to buoyancy-induced convection (as shown for a Questa Mine waste rock dump by Lefebvre et al., 2002).
- The presence of  $\text{CO}_2$  in the dump gas may not be necessary, but it facilitates the equilibrium between dump gas and

atmospheric air densities by allowing the dump gas molar mass to remain close to that of the atmospheric air.

- A coarse-material-filled toe drain and pipe are not necessary, but their presence enhances gas flow, and the pipe poses the main safety threat as it focuses the exit of discharging dump gas.
- Enclosures and topographic depressions bordering the base of a dump, where dense  $O_2$ -deficient dump gas could accumulate, would represent hazard locations.
- The presence of a cover may not be necessary and it could even preclude the type of gas flow observed at the No. 1 Shaft dump. However, covered dumps have limited  $O_2$  supply and may tend to steadily reduce their internal temperatures, which would lead to conditions favorable for the onset of gas flow conditions as observed at the No. 1 Shaft dump.

The conditions listed are not meant to be all inclusive. Further work would be required to assess the full range of conditions that could lead to a gas flow behavior similar to that observed at the No. 1 Shaft dump or to other gas flow behaviors that would also represent a safety threat. This issue is complex because there is a wide range in dump gas composition, waste rock air permeabilities, dump geometries, and atmospheric conditions that could influence gas flow and thus need to be considered. Although the simulation results for the No. 1 Shaft dump shed light on the effect of atmospheric conditions on gas flow in waste rock dumps, it provides a single case study. Similar instrumentation at other sites could provide indications of gas flow behavior departing from the one observed and simulated at the study site. Hockley et al. (2009) further addressed the question of whether hazards such as the one that occurred at the No. 1 Shaft dump are likely to occur at other waste rock dumps. A summary of all the work and conclusions of the technical panel that studied the incident was provided by the Sullivan Mine Incident Technical Panel (2010), including conclusions related to the potential occurrence of similar conditions at other sites.

## Acknowledgments

Teck Cominco is acknowledged for sponsoring the work presented in this paper and granting permission to publish. Walter Kuit of Teck Cominco and Mike O'Kane of O'Kane Consultants are thanked for reviewing an early manuscript of this paper. A NSERC Discovery Grant to R. Lefebvre supported the doctoral research of Belkacem Lahmira, which included the work reported in this paper. We would finally like to thank three anonymous reviewers who provided very constructive and detailed comments that led to considerable improvements of the paper.

## References

- Amos, R.T., D.W. Blowes, L. Smith, and D.C. Sego. 2009. Measurement of wind-induced pressure gradient in a waste rock pile. *Vadose Zone J.* 8:953–962. doi:10.2136/vzj2009.0002
- Anne, R.D., and G. Pantelis. 1997. Coupled natural convection and atmospheric wind forced advection in above ground reacting heaps. In: *Proceedings of the International Conference on Computational Fluid Dynamics in Mineral and Metal Processing and Power Generation*, Melbourne, Australia. 3–4 July 1997. CSIRO, Clayton South, VIC, Australia. p. 453–458.
- Bailey, B.L., L.J.D. Smith, D.W. Blowes, C.J.A. Ptacek, L. Smith, and D.C. Sego. 2013. The Diavik Waste Rock Project: Persistence of contaminants from blasting agents in waste rock effluent. *Appl. Geochem.* 36:256–270. doi:10.1016/j.apgeochem.2012.04.008
- Cathles, L.M., and W.J. Schlitt. 1980. A model of the dump leaching process that incorporates oxygen balance, heat balance, and two dimensional air convection. In W.J. Schlitt and D.A. Shock, editors, *Proceedings of the Las Vegas Symposium on Leaching and Recovering Copper from As-Mined Materials*, Las Vegas, NV. 26 Feb. 1980. Soc. Min. Eng., Englewood, CO. p. 9–27.
- Chi, X., R.T. Amos, M. Stastna, D.W. Blowes, D.C. Sego, and L. Smith. 2013. The Diavik Waste Rock Project: Implications of wind-induced gas transport. *Appl. Geochem.* 36:246–255. doi:10.1016/j.apgeochem.2012.10.015
- Dawson, B., M. Phillip, and M. O'Kane. 2009. Sullivan Mine fatalities incident: Site setting, acid rock drainage management, land reclamation and investigation into the fatalities. In: 8th ICARD International Conference on Acid Rock Drainage, Skelleftea, Sweden. 22–26 June 2009. Vol. 3. Swedish Assoc. Mines, Miner., and Metal Prod., Stockholm. p. 1898–1907.
- Fala, O., J.W. Molson, M. Aubertin, and B. Bussi re. 2005. Numerical modelling of flow and capillary barrier effects in unsaturated waste rock piles. *Mine Water Environ.* 24:172–185. doi:10.1007/s10230-005-0093-z
- Finsterle, S., and E.L. Sonnenthal, editors. 2012. TOUGH Symposium 2012. *Comput. Geosci.* 65:1–136.
- Ganot, Y., M.I. Dragila, and N. Weisbrod. 2012. Impact of thermal convection on air circulation in a mammalian burrow under arid conditions. *J. Arid Environ.* 84:51–62. doi:10.1016/j.jaridenv.2012.04.003
- Guo, W. 1993. Numerical simulation of coupled heat transfer and gas flow in porous media with applications to acid mine drainage. Ph.D. diss. Pennsylvania State Univ., University Park.
- Hockley, D., W. Kuit, and M. Phillip. 2009. Sullivan Mine fatalities incident: Key conclusions and implications for other sites. In: 8th ICARD International Conference on Acid Rock Drainage, Skelleftea, Sweden. 22–26 June 2009. Vol. 3. Swedish Assoc. Mines, Miner., and Metal Prod., Stockholm. p. 1877–1887.
- Jaynes, D.B., A.S. Rogowski, and H.B. Pionke. 1984. Acid mine drainage from reclaimed coal strip mines: 1. Model description. *Water Resour. Res.* 20:233–242. doi:10.1029/WR020i002p00233
- Kamai, T., N. Weisbrod, and M.I. Dragila. 2009. Impact of ambient temperature on evaporation from surface-exposed fractures. *Water Resour. Res.* 45:W02417. doi:10.1029/2008WR007354
- Kuang, X., J.J. Jiao, and H. Li. 2013. Review on airflow in unsaturated zones induced by natural forcings. *Water Resour. Res.* 49:6137–6165. doi:10.1002/wrcr.20416
- Kuo, E.Y., and A.I.M. Ritchie. 1999. The impact of convection on the overall oxidation rate in sulfidic waste rock dumps. In: D. Goldsack et al., editor, *Proceedings of Sudbury '99: Mining and the Environment II*, Sudbury, ON, Canada. 13–15 Sept. 1999. Vol. I. Ctr. in Mining and Mining Environ. Res., Laurentian Univ., Sudbury, ON, Canada. p. 211–220.
- Lahmira, B. 2010. Numerical modeling of physical processes affecting the behaviour of waste rock piles producing acid mine drainage. (In French.) Ph.D. diss. INRS, Eau Terre Environnement, Quebec, QC, Canada.
- Lahmira, B., L. Barbour, and M. Huang. 2014. Numerical modeling of gas flow in the Suncor coke stockpile covers. *Vadose Zone J.* 13(1). doi:10.2136/vzj2013.07.0119
- Lahmira, B., and R. Lefebvre. 2008. Numerical modeling of gas flow in the No. 1 Shaft waste rock dump, Sullivan Mine, B.C., Canada. *Res. Rep. R-970*. INRS, Eau Terre Environnement, Quebec, QC, Canada. <http://espace.inrs.ca/553/1/R000970.pdf> (accessed 21 Jan. 2014).
- Lahmira, B., and R. Lefebvre. 2014. Numerical modelling of transfer processes in a waste rock pile undergoing the temporal evolution of its heterogeneous material properties. *Int. J. Min. Reclam. Environ.* doi:10.1080/17480930.2014.889362
- Lahmira, B., R. Lefebvre, M. Aubertin, and B. Bussi re. 2007. Modeling the influence of heterogeneity and anisotropy on physical processes in AMD-producing waste rock piles. In: *Proceedings, Ottawa Geo2007: 60th Canadian Geotechnical Conference and 8th Joint CGS/IAH-CNC Groundwater Conference*, Ottawa, ON, Canada. 21–24 Oct. 2007. Can. Geotech. Soc., Calgary, AB.
- Lahmira, B., R. Lefebvre, D. Hockley, and M. Phillip. 2009. Sullivan mine fatalities incident: Numerical modeling of gas transport and reversals in flow directions. In: 8th ICARD International Conference on Acid Rock Drainage, Skelleftea, Sweden. 22–26 June 2009. Vol. 3. Swedish Assoc. Mines, Miner., and Metal Prod., Stockholm. p. 1888–1897.
- Lefebvre, R. 1994. Characterization and numerical modeling of acid mine drainage in waste rock piles. (In French.) Ph.D. diss. Univ. Laval, Quebec, QC, Canada.
- Lefebvre, R. 1995. Modeling acid mine drainage in waste rock dumps. In: K. Pruess, editor, *Proceedings, TOUGH Workshop '95*, Berkeley, CA. 20–22 Mar. 1995. LBL-37200. Lawrence Berkeley Natl. Lab., Berkeley, CA. p. 239–244.

- Lefebvre, R. 2010. Écoulement multiphase en milieux poreux. Graduate course notes. 7th ed. GEO-9602/GLG-65146. INRS, Eau Terre Environ., Quebec, QC, Canada. <http://www.ete.inrs.ca/rene-lefebvre?r=enseignement> (accessed 22 Sept. 2014).
- Lefebvre, R., and P.J. Gélinas. 1995. Numerical modelling of AMD production in waste rock dumps. In: *Proceedings, Sudbury '95: Mining and the Environment Conference*, Sudbury, ON, Canada. 29 May–1 June 1995. Laurentian Univ., Greater Sudbury, ON, Canada. p. 869–878.
- Lefebvre, R., D. Hockley, J. Smolensky, and P. Gélinas. 2001a. Multiphase transfer processes in waste rock piles producing acid mine drainage: 1. Conceptual model and system characterization. *J. Contam. Hydrol.* 52:137–164. doi:10.1016/S0169-7722(01)00156-5
- Lefebvre, R., D. Hockley, J. Smolensky, and A. Lamontagne. 2001b. Multiphase transfer processes in waste rock piles producing acid mine drainage: 2. Applications of numerical simulations. *J. Contam. Hydrol.* 52:165–186. doi:10.1016/S0169-7722(01)00157-7
- Lefebvre, R., B. Lahmira, and W. Löbner. 2011. Numerical modeling of gas flow to select a radon emission control method in waste rock dump 38neu, Germany. In: *Proceedings of Geohydro 2011, 1st Joint CANQUA/IAH-CNC Conference*, Quebec City, QC, Canada. 28–31 Aug. 2011. Paper 2410.
- Lefebvre, R., B. Lahmira, and W. Löbner. 2012. Field monitoring and numerical modeling of gas flow and radon emission control in waste rock dump 38neu, Germany. In: *8th ICARD International Conference on Acid Rock Drainage*, Skelleftea, Sweden. 22–26 June 2009. Vol. 1. Swedish Assoc. Mines, Miner., and Metal Prod., Stockholm. p. 1432–1442.
- Lefebvre, R., A. Lamontagne, and C. Wels. 2001c. Numerical simulations of acid rock drainage in the Sugar Shack South rock pile, Questa Mine, New Mexico, U.S.A. In: *Proceedings, 2001 an Earth Odyssey: 2nd Joint IAH-CNC and CGS Groundwater Specialty Conference and 54th Canadian Geotechnical Conference*, Calgary, Canada. 16–19 Sept. 2001. Contrib. Ser. 2001043. Geol. Surv. Canada, Ottawa, ON. p. 1568–1575.
- Lefebvre, R., A. Lamontagne, C. Wels, A. Mac, and G. Robertson. 2002. ARD production and water vapor transport at Questa Mine. In: *Tailings and Mine Waste '02, Proceedings of the 9th International Conference on Tailings and Mine Waste*, Fort Collins, CO. 27–30 Jan. 2002. A.A. Balkema Publ., Rotterdam, the Netherlands. p. 479–488.
- Lefebvre, R., J. Smolensky, and D. Hockley. 1998. Modeling of acid mine drainage physical processes in the Nordhalde of the Ronnenburg mining district, Germany. In: *Proceedings, TOUGH Workshop '98*, Berkeley, CA. 4–6 May 1998. Lawrence Berkeley Natl. Lab., Berkeley, CA. p. 228–233.
- Linklater, C.M., D.J. Sinclair, and P.L. Brown. 2005. Coupled chemistry and transport modeling of sulphidic waste rock dumps at the Aitik mine site, Sweden. *Appl. Geochem.* 20:275–293. doi:10.1016/j.apgeochem.2004.08.003
- Lu, N., and Y. Zhang. 1997. Thermally induced gas convection in mine wastes. *Int. J. Heat Mass Transfer* 40:2621–2636.
- Massmann, J., and D.F. Farrier. 1992. Effects of atmospheric pressures on gas transport in the vadose zone. *Water Resour. Res.* 28:777–791. doi:10.1029/91WR02766
- Massman, W.J., and J.M. Frank. 2006. Advective transport of CO<sub>2</sub> in permeable media induced by atmospheric pressure fluctuations: 2. Observational evidence under snow packs. *J. Geophys. Res.* 111:G03005.
- Moghtaderi, B., B.Z. Dlugogorski, and E.M. Kennedy. 2000. Effects of wind flow on self-heating characteristics of coal stockpiles. *Process Saf. Environ. Prot.* 78:445–453. doi:10.1205/095758200530998
- Molson, J.W., O. Fala, M. Aubertin, and B. Bussière. 2005. Numerical simulations of pyrite oxidation and acid mine drainage in unsaturated waste rock piles. *J. Contam. Hydrol.* 78:343–371. doi:10.1016/j.jconhyd.2005.06.005
- Nachshon, U., M.I. Dragila, and N. Weisbrod. 2012. From atmospheric winds to fracture ventilation: Cause and effect. *J. Geophys. Res.* 117:G02016.
- Nachshon, U., N. Weisbrod, and M.I. Dragila. 2008. Quantifying air convection through surface-exposed fractures: A laboratory study. *Vadose Zone J.* 7:948–956. doi:10.2136/vzj2007.0165
- Neeper, D.A. 2002. Investigation of the vadose zone using barometric pressure cycles. *J. Contam. Hydrol.* 54:59–80. doi:10.1016/S0169-7722(01)00146-2
- Neeper, D.A. 2003. Harmonic analysis of flow in open boreholes due to barometric pressure cycles. *J. Contam. Hydrol.* 60:135–162. doi:10.1016/S0169-7722(02)00086-4
- Neeper, D.A., and P. Stauffer. 2005. Unidirectional gas flow in soil porosity resulting from barometric pressure cycles. *J. Contam. Hydrol.* 78:281–289. doi:10.1016/j.jconhyd.2005.06.001
- Neuner, M., L. Smith, D.W. Blowes, D.C. Sego, L.J.D. Smith, and M. Gupton. 2013. The Diavik Waste Rock Project: Water flow through waste rock in a permafrost terrain. *Appl. Geochem.* 36:222–233. doi:10.1016/j.apgeochem.2012.03.011
- Pantelis, G., and A.I.M. Ritchie. 1992. Rate-limiting factors in dump leaching of pyritic ores. *Appl. Math. Model.* 16:553–560. doi:10.1016/0307-904X(92)90005-N
- Pham, N., D.C. Sego, L.U. Arenson, D.W. Blowes, R.T. Amos, and L. Smith. 2013. The Diavik Waste Rock Project: Measurement of thermal regime in a waste rock pile under permafrost environment. *Appl. Geochem.* 36:234–245.
- Phillip, M., D. Hockley, B. Dawson, W. Kuit, and M. O'Kane. 2009. Sullivan Mine fatalities incident: Technical investigations and findings. In: *8th ICARD International Conference on Acid Rock Drainage*, Skelleftea, Sweden. 22–26 June 2009. Vol. 3. Swedish Assoc. Mines, Miner., and Metal Prod., Stockholm. p. 1908–1918.
- Pruess, K. 1991. TOUGH2: A general purpose numerical simulator for multiphase fluid and heat transfer. LBL-29400. Lawrence Berkeley Natl. Lab., Berkeley, CA.
- Pruess, K., C.M. Oldenburg, and G.J. Moridis. 2012. TOUGH2 user's guide, Version 2. Revised ed. Rep. LBNL-43134. Lawrence Berkeley Natl. Lab., Berkeley, CA. [http://esd.lbl.gov/files/research/projects/tough/documentation/TOUGH2\\_V2\\_Users\\_Guide.pdf](http://esd.lbl.gov/files/research/projects/tough/documentation/TOUGH2_V2_Users_Guide.pdf) (accessed August 2014).
- Ritchie, A.I.M., and P. Miskelly. 2000. Geometric and physico-chemical properties determining sulfide oxidation rates in waste rock dumps. In: *Proceedings of the 5th International Conference on Acid Rock Drainage, ICARD-2000*, Denver, CO. 21–24 May 2000. Soc. Min. Metall. Explor., Littleton, CO. p. 277–287.
- Smith, L.J.D., B.L. Bailey, D.W. Blowes, J.L. Jambor, L. Smith, and D.C. Sego. 2013a. The Diavik Waste Rock Project: Initial geochemical response from a low sulfide waste rock pile. *Appl. Geochem.* 36:210–221. doi:10.1016/j.apgeochem.2012.06.008
- Smith, L.J.D., D.W. Blowes, J.L. Jambor, L. Smith, D.C. Sego, and M. Neuner. 2013b. The Diavik Waste Rock Project: Particle size distribution and sulfur characteristics of low-sulfide waste rock. *Appl. Geochem.* 36:200–209. doi:10.1016/j.apgeochem.2013.05.006
- Smith, L.J.D., M.C. Moncur, M. Neuner, M. Gupton, D.W. Blowes, L. Smith, and D.C. Sego. 2013c. The Diavik Waste Rock Project: Design and construction of field-scale instrumented waste rock piles. *Appl. Geochem.* 36:187–199. doi:10.1016/j.apgeochem.2011.12.026
- Smolensky, J., D. Hockley, R. Lefebvre, and M. Paul. 1999. Oxygen transport processes in the Nordhalde of the Ronnenburg mining district, Germany. p. 271–280. In: D. Goldsack et al., editor, *Proceedings of Sudbury '99: Mining and the Environment II*, Sudbury, ON, Canada. 13–15 Sept. 1999. Vol. 1. Ctr. in Mining and Mining Environ. Res., Laurentian Univ., Sudbury, ON, Canada. p. 271–280.
- Srcek, O., M. Choquette, P. Gélinas, R. Lefebvre, and R.V. Nicholson. 2004. Geochemical characterization of acid mine drainage from a waste rock pile, Mine Doyon, Québec, Canada. *J. Contam. Hydrol.* 69:45–71. doi:10.1016/S0169-7722(03)00150-5
- Sullivan Mine Incident Technical Panel. 2010. Sullivan Mine fatalities: Technical investigations, summary report. Ministry of Energy, Mines and Petroleum Resources, Victoria, BC, Canada.
- Weeks, E.P. 1979. Field determination of vertical permeability to air in the unsaturated zone. Prof. Pap. 1051. USGS, Reston, VA.
- Weisbrod, N., and M.I. Dragila. 2006. Potential impact of convective fracture venting on salt-crust buildup and ground-water salinization in arid environments. *J. Arid Environ.* 65:386–399. doi:10.1016/j.jaridenv.2005.07.011
- Weisbrod, N., M.I. Dragila, U. Nachshon, and M. Piliersdorf. 2009. Falling through the cracks: The role of fractures in Earth-atmosphere gas exchange. *Geophys. Res. Lett.* 36:L02401. doi:10.1029/2008GL036096
- Wels, C., R. Lefebvre, and A.M. Robertson. 2003. An overview of prediction and control of air flow in acid-generating waste rock dumps. In: *Proceedings, 6th International Conference on Acid Rock Drainage (ICARD)*, Cairns, Australia. 12–18 July 2003. AusIMM, Carlton South, VIC, Australia. p. 639–650.
- Wu, Y., K. Zhang, and H. Liu. 2006. Estimating large-scale fracture permeability of unsaturated rock using barometric pressure data. *Vadose Zone J.* 5:1129–1142. doi:10.2136/vzj2006.0015